3.2 PROCESS DEVELOPMENT AND OPTIMIZATION FOR SILICON CARBIDE JOINING AND IRRADIATION STUDIES-IV— Takaaki Koyanagi, James Kiggans, Chunghao Shih, Yutai Katoh (Oak Ridge National Laboratory)

OBJECTIVE

The objective of this task is to develop and optimize joining processes for silicon carbide (SiC) ceramics and its composites for fusion energy applications.

SUMMARY

Processing and characterization of SiC ceramics joined by the pressureless transient eutectic-phase (PL-TEP) method were conducted. Apparent shear strengths of ~100 MPa was demonstrated by torsion test on the PL-TEP joint formed with SiC nano-powder, oxide additives, and organic agents. The fracture behavior was typical of robust joints. In addition, the joints are expected to have high densities based on sintered densities of monolithic SiC representing the PL-TEP joint layer. Irradiation of SiC joints made with different bonding materials is being conducted in HFIR.

PROGRESS AND STATUS

Introduction

The development of SiC joints that retain adequate mechanical and functional properties in a fusion reactor environment is essential for the use of SiC and its composites as the primary structural material [1]. Effects of neutron irradiation on the material performance are among the most critical factors in a fusion reactor environment. TEP method, which is a specific type of liquid phase sintering, is one of the fabrication routes used to obtain dense and radiation-resistant SiC-matrix composites [2, 3]. The TEP process involves the use of SiC nano-powder and a reduced amount of sintering additives such as the yttrium-alumina system. The TEP process is also used to join SiC ceramics [4].TEP joining is attractive for nuclear application because this joining method can provide SiC base joint layer with dense microstructures, high strengths, and expected irradiation tolerance. In fact, a pressurized TEP process was used to join SiC materials, and the excellent irradiation-tolerance and adequate shear strength was demonstrated following neutron irradiation at low to intermediate fluence [5]. However, requirement of the external pressure during heat treatment is a major factor that dictates applicability of a specific joining method to integration of components with large sizes and complex geometries. To overcome this problem, previous work demonstrated feasibility of robust PL-TEP joining without the use of loads during heat treatment [6]. Present work presents processing and characterization of PL-TEP joints to optimize the processing.
This report also provides current progress of the neutron irradiation experiments in HFIR.

Experimental Procedure

Materials

The PL-TEP joints were formed using the powder mixtures consisting of SiC nano-powder (average diameters ~30 nm) or combined SiC nano- and micron-powders, and sintering additives (Al_2O_3 powder and Y_2O_3 powder), with or without organic agents such as Polyvinylpyrrolidone (PVP) and acrawax. The total amount of the oxide additives was 6 or 10 wt.%. The total amount of the organic agents was ~3.5 wt.%. The PL-TEP joints were formed by sandwiching mixed powder between chemical vapor deposited (CVD) plates followed by cold-pressing at ~10 MPa in graphite die to partially densify the powder. The sandwiched materials were then heat-treated at 1875°C for 1 h in a flowing argon atmosphere in the graphite die without external loading. The dimension of the pair of CVD SiC plates was 21.0 mm (w) ×

31.2 cm (l) × 6.2 mm (t). Process conditions and specimen ID are summarized in Table 1. This is updated table as was shown in a previous report [6].

PL-TEP SiC monoliths, representing the bonded layer of the PL-TEP joints, were also fabricated to estimate density of the joint layers. The feedstock of the monolithic forms was the same as that used for the PL-TEP joints, except for additional use of carbowax as an organic agent for pressing the compacts. A steel die was used for cold pressing of the test pellets. The typical SiC monolithic cylindrical pellets before sintering had dimensions ~8 mm diameter and ~10mm thickness. The sintering was performed at 1875°C for 1 h in a flowing argon atmosphere. Density measurements were conducted by weighting and measuring before sintering and by Archimedes density measurement after sintering. Specimen ID and processing conditions for the PL-TEP SiC is listed in Table 2.

Table 1**.** Processing conditions, apparent shear strength, and fracture behavior of CVD-SiC joined by PL-TEP method.

Material	**Specimen ID**	**Alias**	**Processing Conditions**				**Joint Strength**			
			Starting Materials	Atm.	Temp. (^{o}C)	Time (h)	Test method	Apparent shear strength (MPa) [1]	Fracture location	# of tests
PL-TEP joint	TEP-6A	RUN 34	SiC nano and micron powder, 6wt.% oxide additives, 3.5 wt% PVP and acrawax	Ar	1875	1	DNS [2]	113±52	Joint layer	3
	TEP-6B	RUN 36	SiC nano powder, 6wt.% oxide additives, 3.5 wt% PVP and acrawax	Ar	1875	1	DNS	163±43	Substrate	3
		RUN 37C					Torsion	104±23	Substrate	4
	TEP-6C	RUN 35	SiC nano powder, 6wt.% oxide additives,	Ar	1875	1	N.D. [3]			
	TEP-10B	RUN 38	SiC nano powder, 10wt.% oxide additives, 3.5 wt% PVP and acrawax	Ar	1875	1	DNS	224±18	Substrate	3

[1] Average strength ±one standard deviation
[2] Double notch shear test
[3] Not determine

Table 2. Processing conditions and apparent density of PL-TEP SiC monoliths.

Material	Specimen ID	Starting materials	Apparent Density Before Sintering (%)	Apparent Density After Sintering (%)
Pressureless TEP SiC	P53a	Same for TEP-6B	31.70	94.73
	P53b	SiC nano-powder, 6 wt.% oxide additives, 3.5wt.% acrawax and carbowax	30.33	93.38
	P57	SiC nano-powder, 10 wt.% oxide additives, without organic agents	29.07	95.89
	P57a	Same for TEP-10B	28.91	94.20
	P57b	SiC nano-powder, 10 wt.% oxide additives, 3.5wt.% acrawax and carbowax	31.07	96.38

Shear strength determination

The shear strengths of the SiC joints were determined by double-notch shear (DNS) test [7] and torsional shear test. The DNS test was used for a quick estimation of the shear strength due to the ease of specimen preparation, and the torsion test was used for a more accurate strength evaluation because this test can provide uniform stress states at the joints. Details of the DNS test used in this work can be found elsewhere [6]. The dimensions of the torsional test specimen were 6 mm × 6 mm × 3 mm, with the diameter of the neck 4 mm as shown in Figure 1. The torsional test was conducted using TestResources 160GT-125Nm torsion system with flexible couplers and sample grips (Figure 2). Aluminum-alloy tabs were installed at the square grip sections to obtain uniform stress distributions there. The rotation speed was 0.15 deg/min. Nominal shear strength values (τ) in this work are given by following equation,

$$\tau = 16T/\pi d^3 \qquad (1)$$

where T is the applied torque and d is the specimen diameter of the neck. Number of the torsion tests was four. Further description of details of the test method can be found elsewhere [8]. All mechanical tests were conducted at room temperature.

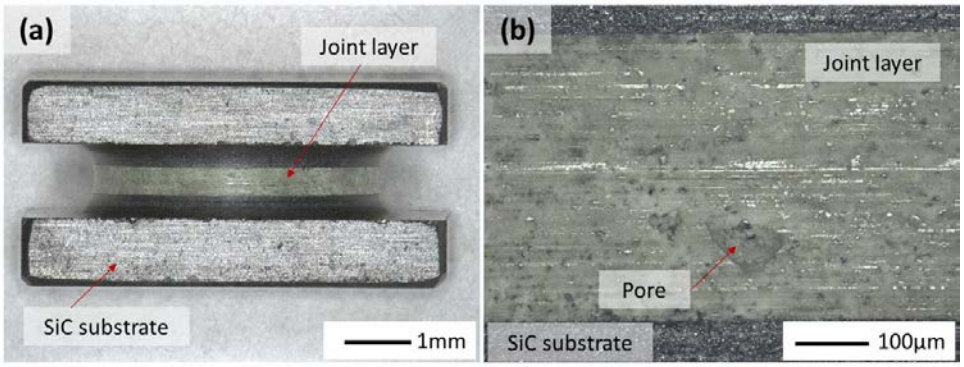

Figure 1. Optical micrograph of the torsional test specimen of PL-TEP joint:
(a) Side-view image, and (b) magnified images of the joint region.

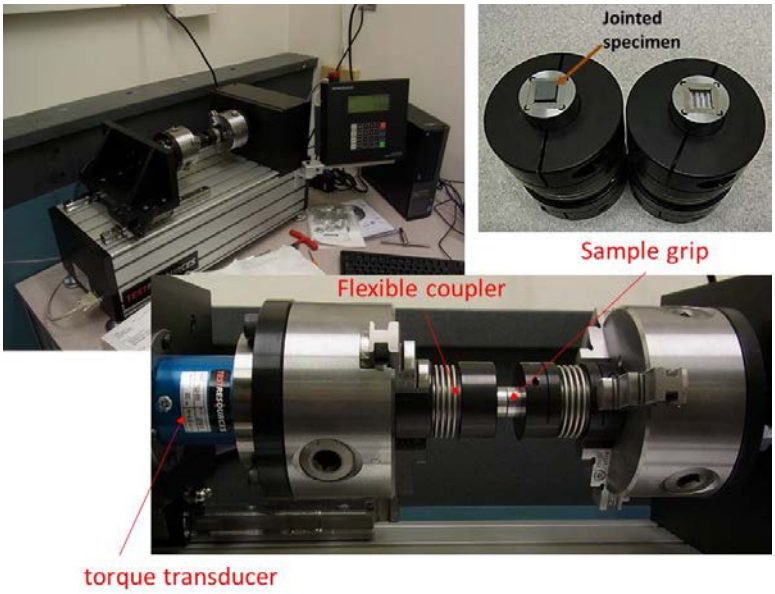

Figure 2. Overview of the torsional testing machine.

Metallographic examinations

Microstructures of the bonded regions were characterized using optical microscope (Keyence, VHX-1000) and field-emission scanning electron microscope (SEM, Hitachi, S4800) equipped with energy dispersive spectroscopy (EDS).

Results

Shear strength investigation of PL-TEP joints

The DNS tests on the TEP-10B joints and the torsion tests on the TEP-6B joints were conducted. The average DNS strengths and the one standard deviation of the TEP-10B joint were 224 and 18 MPa, respectively. The cracks ran through the SiC substrates based on the observation of the tested

specimens. The apparent DNS strength of over 150 MPa and the substrate failure observed in the TEP-10B were typical for a strong joint as observed in the TEP-6B joint and metallic diffusion-bonded SiC joints [6, 9].
For the torsion specimen, ~50 µm sized pores was observed on the surface of bonded zone of the TEP-6B joint (Figure 1 (b)). The apparent shear strengths of ~100 MPa were demonstrated by the torsional test with that joint. The bonded zone of the specimen got shattered into pieces after the test. Visual observations of the fractured areas show that the cracks ran through both the joint layer and SiC substrates as shown in Figure 3. The failure within the SiC base material was typically observed in robust SiC joints determined by the torsional shear test on hourglass specimens [5].

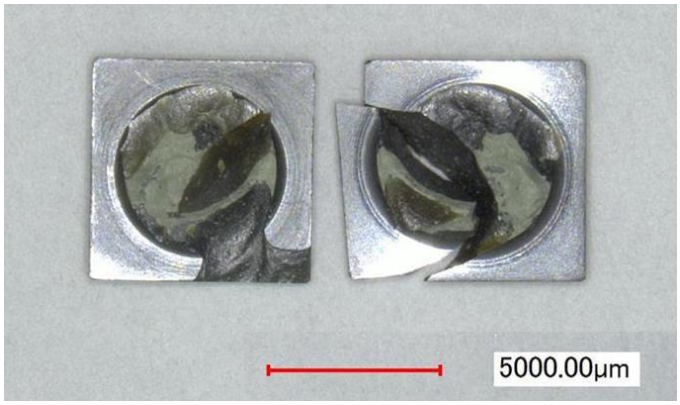

Figure 3. Photograph of pieces of the torsional tested specimens

To understand the fracture behavior, crack observations were conducted using optical microscopy on the partially broken torsion tested samples, as shown in Figure 4. Note that the torsion test was stopped after detection of ~30% decreased in applied torque during the testing. The apparent shear strength of the torsion “tested” sample was very weak (~10 MPa). The crack ran through the SiC substrate and bonded zone as shown in Figure 4. The crack near the joint region typically runs at an angle of approximately 45° to joint interface, which appeared to be perpendicular to the tensile stress component in the shear-loaded specimen. It was difficult to identify the crack initiation site, but the stress state during the testing suggests the possible initiation site is surface defects of bonded zone such as pre-existing pores, [4].

In summary of shear strength determinations, both TEP-6B and 10B joints exhibited a fracture behavior characteristic of robust joints. This indicates that both joints are promising from the point of view of strength.

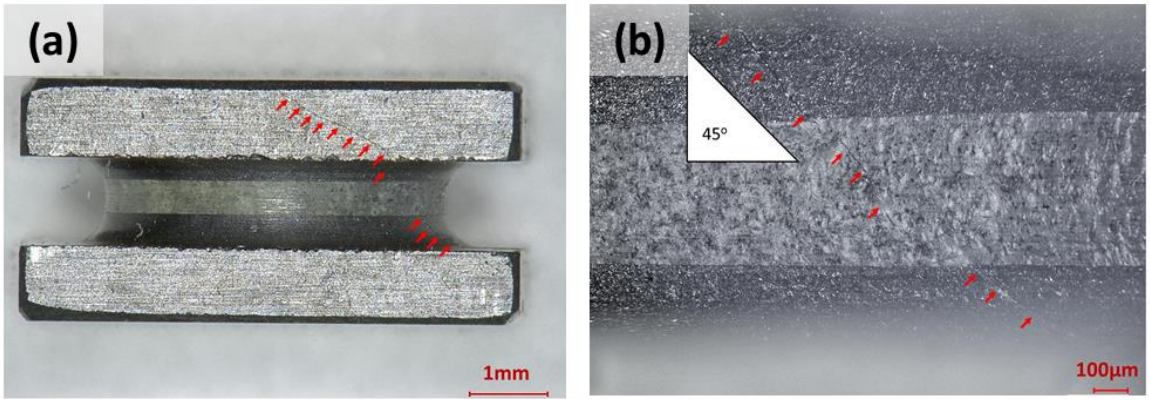

Figure 4. Micrographs of torsion tested PL-TEP joint (TEP-6B): (a) low-magnification image, and (b) high-magnification image. Cracks caused by the torsion test are arrowed.

Processing and characterization of PL-TEP SiC monolith

Due to the difficulty of accurate density measurement of the joint layer, the apparent densities of the PL-TEP SiC in pellet form were performed. Results of the density measurements are summarized in Table 2. The data of the PL-TEP SiC with 6 wt.% oxides and without organic agent is absent because of chipping of the weak powder-compact before sintering. Relative densities before and after sintering were ~30% and ~95%, respectively, for all samples. The effect of the amount of oxide additives on the density of the PL-TEP SiC was insignificant in this work. In addition, the effect of organic agents on the density was not clear.
SEM images of the PL-TEP SiC are shown in Figure 5. Pores with a few tens micron size were observed in the PL-TEP SiC with 6 wt.% oxides and 3.5 wt.% organic agents. The size of pore was decreased by use of 10 wt.% oxide additives and 3.5 wt.% organic agents. The pore size was the smallest in case of the PL-TEP SiC without organic agents, while the difference of the densities between the PL-TEP SiC pellets was not significant.

The results of the density measurements and the microstructural observations provide the following implications: (1) organic agents caused the large pore, and (2) increased amount of the oxide additives reduced the pore size. However, note that the organic agents are necessary during the cold pressing to form robust PL-TEP joints, as indicated in previous work [6]. The use of the organic agents represents a trade-off between the addition of pores and the needed strength provided to the pre-sintered materials. More work may be needed to investigate the effect of the organic agents. In summary, high density (~95% relative density) is potentially expected for the bonded zone of PL-TEP joints with both 6 and 10 wt.% oxide additives, though the amount of oxide additives and use of the organic agents affected the morphology of pore structure.

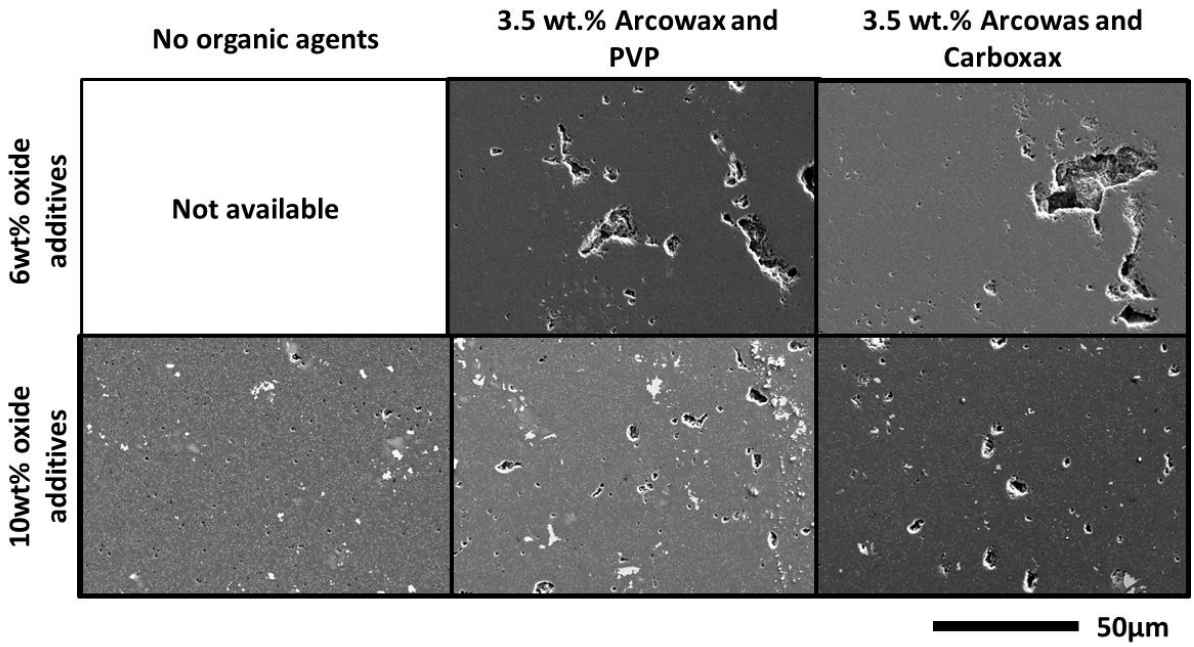

Figure 5. Secondary electron images of the various PL-TEP SiC.

Current progress of neutron irradiation experiments

Rabbit capsules containing SiC joint specimens are being irradiated in HFIR to study effects of neutron irradiation on the shear strength. Five capsules containing a total of 80 samples are being irradiated under three different irradiation conditions. The materials and the irradiation conditions are summarized in Table 3 and 4. The target irradiation conditions are: 500°C to 3 dpa, 500°C to 10 dpa, and 1000°C to 3 dpa. The bonded material is high-purity CVD SiC. The joints were fabricated by pressureless or pressurized methods. The pressureless joined materials are MAX phase joints provided by Rolls-Royce HTC and ORNL, PL-TEP joints by ORNL, and CA glass ceramics joints by Politecnico di Torino. The pressurized-method joined materials are metallic diffusion-bonding using Ti and Mo by ORNL, MAX phase tape casting by PNNL, spark plasma sintering (SPS) by Queen Mary University of London, and TEP using slurry and tape casting by Kyoto University. The joint phases nominally include Ti-Si-C system in the Ti diffusion and the MAX phase joints, metallic Ti in the SPS joint, SiC with Y-Al oxide phases in the TEP joints, Mo-Si-C system in the Mo diffusion joint, and calcia-alumina glass in the glass ceramic joint. Regarding post-irradiation experiments, torsional tests using the Test Resources 160GT-125Nm torsion system is planned. Observation of the fracture appearance will also be conducted. In addition the actual irradiation temperatures will be evaluated by dilatometry of CVD SiC temperature monitors that are internal components of the capsules containing the SiC joints. Torsion tests on control specimens are ongoing.

Table 3.Irradiation test matrix for various SiC joints.
The checks denote test conditions planned in this work.

Joining Method	Expected Joint Phases	Provider	Target Irradiation Conditions		
			500C 3dpa	500C 10dpa	1000C 3dpa
Ti diffusion	Ti_3SiC_2, TiC	ORNL	√		√
Pressureless MAX phase	Ti_3SiC_2, SiC	Rolls-Royce HTC/ORNL	√		√
MAX phase	Ti_3SiC_2, SiC	PNNL		√	
New MAX phase	MAX phase	PNNL	√		
Ti SPS	Ti	Queen Mary University	√		
Pressureless TEP	SiC, Y-Al-O	ORNL	√		√
TEP slurry	SiC, Y-Al-O	Kyoto University		√	√
TEP tape	SiC, Y-Al-O	Kyoto University		√	√
Mo diffusion	Mo_5Si_3C, Mo_2C	ORNL	√		√
CA glass	$12CaO{\cdot}7Al_2O_3$, $3CaO{\cdot}Al_2O_3$	Politecnico di Torino		√	√

Table. 4 Irradiation conditions for HFIR rabbit capsules containing various SiC joints.

Rabbit ID	Rabbit ID2	TEMPERATURE (°C)	HFIR POSITION		TARGET FLUENCE (10^{21} n/cm^2)	FAST FLUX (n/cm^2-s)	NUMBER OF CYCLES	FAST FLUENCE PER CYCLE (n/cm^2)	EXPECTED TOTAL FLUENCE (n/cm^2)
SCJ2-10	FTS1	500	TRRH	7	3	7.00E+14	2	1.45E+21	2.90E+21
SCJ2-11	FTS3	500	TRRH	7	10	7.00E+14	7	1.45E+21	1.02E+22
SCJ2-12	FTS2	500	TRRH	7	3	7.00E+14	2	1.45E+21	2.90E+21
SCJ2-16	FTS4	1000	PTP	5	3	1.11E+15	1	2.30E+21	2.30E+21
SCJ2-17	FTS5	1000	PTP	5	3	1.11E+15	1	2.30E+21	2.30E+21

REFERENCES

[1] Y. Katoh, L.L. Snead, I. Szlufarska, W.J. Weber, J. Nucl. Mater., 16 (2012) 143.
[2] Y. Katoh, S.M. Dong, A. Kohyama, Fusion Eng. Des., 61–62 (2002) 723.
[3] T. Koyanagi, K. Ozawa, T. Hinoki, K. Shimoda, Y. Katoh, J. Nucl. Mater., 448 (2014) 478.
[4] H.-C. Jung, T. Hinoki, Y. Katoh, A. Kohyama, J. Nucl. Mater., 417 (2011) 383.
[5] Y. Katoh, L.L. Snead, T. Cheng, C. Shih, W.D. Lewis, T. Koyanagi, T. Hinoki, C.H. Henager Jr., M. Ferraris, J. Nucl. Mater., 448 (2014) 497.
[6] T. Koyanagi, J.O. Kiggans, T. Cheng, Y. Katoh, Fusion Materials Semiannual Progress Report for Period Ending December 31, 2013, DOE/ER-0313/55, U. S. Department of Energy, 22.
[7] ASTM C1292-10, (2010).
[8] H.-C. Jung, T. Hinoki, Y. Katoh, A. Kohyama, J. Nucl. Mater., 417 (2011) 383.
[9] T. Koyanagi, J. Kiggans, C. Shih, Y. Katoh, Proceedings of 38th Int'l Conf & Expo on Advanced Ceramics & Composites (ICACC 2014), Manuscript ID: 1789424.R1.